HHS Public Access

Author manuscript

Chem Res Toxicol. Author manuscript; available in PMC 2023 February 21.

Published in final edited form as:

Chem Res Toxicol. 2022 February 21; 35(2): 254–264. doi:10.1021/acs.chemrestox.1c00309.

Formation of redox-active duroquinone from vaping of vitamin E acetate contributes to oxidative lung injury

Alexa Canchola[1], **C.M. Sabbir Ahmed**[1], **Kunpeng Chen**[2], **Jin Y. Chen**[1], **Ying-Hsuan Lin**[1,2,*]

[1]Environmental Toxicology Graduate Program, University of California, Riverside, CA, USA

[2]Department of Environmental Sciences, University of California, Riverside, CA, USA

Abstract

In late 2019, the outbreak of e-cigarette, or vaping-associated lung injuries (EVALI) in the United States demonstrated to the public the potential health risks of vaping. While studies since the outbreak have identified vitamin E acetate (VEA), a diluent of tetrahydrocannabinol (THC) in vape cartridges, as a potential contributor to lung injuries, the molecular mechanisms through which VEA may cause damage are still unclear. Recent studies have found the thermal degradation of e-liquids during vaping can result in the formation of products that are more toxic than the parent compounds. In this study, we assessed the role of duroquinone (DQ) in VEA vaping emissions that may act as a mechanism through which VEA vaping causes lung damage. VEA vaping emissions were collected and analyzed for their potential to generate reactive oxygen species (ROS) and induce oxidative stress-associated gene expression in human bronchial epithelial cells (BEAS-2B). Significant ROS generation by VEA vaping emissions were observed in both acellular and cellular systems. Furthermore, exposure to vaping emissions resulted in significant upregulation of *NQO1* and *HMOX-1* genes in BEAS-2B cells, indicating a strong potential for vaped VEA to cause oxidative damage and acute lung injury; the effects are more profound than exposure to equivalent concentrations of DQ alone. Our findings suggest there may be synergistic interactions between thermal decomposition products of VEA, highlighting the multifaceted nature of vaping toxicity.

Graphical Abstract

[*]**Corresponding Author Ying-Hsuan Lin** - Department of Environmental Sciences, University of California, Riverside, California 92521, United States; Environmental Toxicology Graduate Program, University of California, Riverside, California 92521, United States; Phone: +1-951-827-3785, ying-hsuan.lin@ucr.edu.

Alexa Canchola – Environmental Toxicology Graduate Program, University of California, Riverside, California 92521, United States

C.M. Sabbir Ahmed – Environmental Toxicology Graduate Program, University of California, Riverside, California 92521, United States

Kunpeng Chen – Department of Environmental Sciences, University of California, Riverside, California 92521

Jin Y. Chen – Environmental Toxicology Graduate Program, University of California, Riverside, California 92521, United States

Supporting Information

Temperature profile of vape pen battery during activation (Figure S1); experimental setup for VEA vaping emission collection (Figure S2); gene expression of *HMOX*-1 and *NQO1* collected at 0, 3, 6, 12, and 24 hr (Figure S3); experimental set up for particle volume and number collection efficiency (Figure S4); experimental set up and cut size verification for MOUDI particle collection (Figure S5); total and extracted ion chromatograms of polar VEA vaping emissions analyzed on GC/MS (Figure S6); total and extracted ion chromatograms of non-polar polar VEA vaping emissions analyzed on GC/MS (Figure S7); DCF reaction scheme (Figure S8); time series of acellular and cellular $DCFH_2$ oxidation (Figure S9).

The authors declare no competing financial interest.

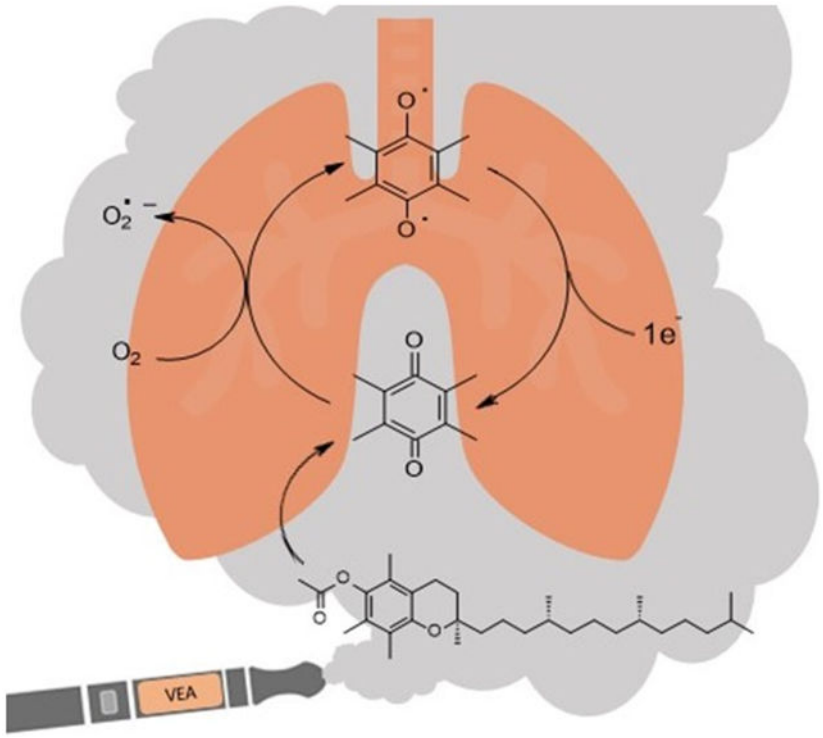

1. Introduction

Vaping, or inhalation of aerosolized e-cigarette liquids, has become increasingly popular over the last decade, particularly among adolescents and those trying to quit tobacco cigarettes.[1] The popularity of vaping has largely been attributed to the customization options available (through both the e-cigarette design and liquid flavors) as well as their perception as a safer alternative compared to traditional cigarettes.[2] However, the outbreak of the vaping-related illness, known as EVALI (e-cigarette, or vaping, product use-associated lung injury), in users of e-cigarettes and vaping products highlights the potential contribution of vaping to public health risks.

The wave of vaping-related injuries began in August of 2019 and by February of 2020, the Centers for Disease Control and Prevention (CDC) had reported over 2,800 hospitalizations of patients who displayed symptoms of coughing, dyspnea (shortness of breath), and chest pain characteristic of acute respiratory distress syndrome.[3] Majority of affected patients appeared to be young (under 35), with no history of pre-existing respiratory conditions that may have caused the damage.[4, 5] Majority of patients did, however, report the use of e-cigarette or vape products within 3 months preceding the onset of any symptoms.[5] Over 80% of surveyed patients reported that they had used tetrahydrocannabinol (THC)-containing vaping products, and 35% used THC exclusively.[4, 5] Evidence suggests that vitamin E acetate (VEA), found in high frequency in illicit cannabinoid-containing vaping cartridges and in the bronchoalveolar lavage of EVALI patients, are strongly linked to the outbreak.[6, 7] However, the exact causative agents and underlying molecular mechanisms remain unclear.

VEA is a synthetic derivative of vitamin E used in black market or homemade vaping cartridges as a viscosity enhancer to dilute or “cut” THC. In some instances, the ratio of VEA to THC in cartridges linked to EVALI cases was found to be greater than 95%.[7] Alone, vitamin E and its derivatives are considered safe for consumption and are often used in skin-care products for protection against UV-induced damage.[8] However, recent studies have demonstrated that VEA and other e-liquids undergo drastic changes in chemical composition during the vaping process, forming products such as formaldehyde, acrolein, acetaldehyde, and more depending on the oil heated.[9-11] Vaping of VEA in particular was found to result in the formation of the reactive quinone species, duroquinone (DQ).[7, 10, 11]

Quinones like DQ are highly redox active molecules that can undergo redox cycling – a process in which the quinone is reduced by a cellular reductase (such as NADPH quinone reductase) or reducing agent to a semiquinone radical.[12, 13] This radical can then react with molecular oxygen to produce superoxide and re-form the quinone, resulting in the generation of reactive oxygen species (ROS), including superoxide, hydrogen peroxide, and hydroxyl radicals.[14] The redox cycling can continue indefinitely until oxygen or a reducing agent concentration has been depleted, which ultimately leads to oxidative stress and damage to crucial molecules including lipids, proteins, and DNA.[14] In addition to ROS-mediated damage, quinones can act as electrophiles capable of direct damage via Michael addition to macromolecules such as DNA and proteins.[14, 15] Many studies have indicated that inhalation of various quinone species can lead to detrimental effects on human lung health, especially to airway epithelium.[15-17]

To date, few studies have investigated the potential role of the thermal degradation products of VEA in acute lung injuries. For this reason, the objective of this study was to assess the potential of DQ produced during VEA vaping to induce oxidative damage in human airway epithelial cells as a possible contributing factor. VEA vaping emissions were analyzed using gas chromatography/mass spectrometry (GC/MS) methods and applied to human airway epithelial cells (BEAS-2B) to assess oxidative potential and toxicological responses upon exposure. Additionally, we investigated the size distribution of vaping aerosols and the chemical constituents at different size fractions to characterize the potential risk of aerosol lung deposition.

2. Materials and Methods

2.1 Materials

DL-alpha tocopherol acetate (VEA, > 97%), DL-alpha tocopherol (vitamin E, > 97%), tetramethyl-1,4-benzoquinone (DQ, > 98%), durohydroquinone (DHQ, > 95%), tert-butyl hydroperoxide (TBHP, 70% in water), and sodium hydroxide (NaOH, 1.0 M in water) were purchased from Tokyo Chemical Industry (TCI America, Inc.). 1, 3, 5-trichlorobenzene (TCB, 98%) was purchased from Alfa Aesar. Acetonitrile (ACN, 99.95%) was purchased from Fisher Chemical. Triton X-100 (10% w/v) was purchased from Roche. Cell-grade dimethyl sulfoxide (DMSO) was purchased from MP Biomedicals. 2’-7’-dichlorodihydrofluorescein diacetate ($DCFH_2DA$) was purchased from Cayman Chemical Company. Phosphate Buffered Saline (PBS, 1X) was purchased from Corning. Fluoro-Max™ Green Fluorescent Microspheres (0.27 μm) were purchased from Thermo Scientific.

2.2 Sample Collection

The procedure for collecting VEA vaping aerosols was adapted from previous studies[10, 11, 18] to maintain reproducibility with other e-cigarette research. The vape pen (CCell M3b) was operated at 3.6 V. The average peak temperature of the heating element was measured to be 218.6 ± 3.6 °C using a 1 mm grounded k-type thermocouple wire (MN Measurement Instruments) following the protocol previously described in Chen et al.[19] (Figure S1). The full protocol for the measurement of the heating element temperature is described in the Supporting Information (SI).

A fresh cartridge (CCell TH2; 0.5 mL, 2.2 Ω) was used for each collection. Prior to each collection, the cartridge was filled with VEA standard oil, weighed, and preconditioned by taking 3-5 puffs until the oil was properly warmed. Vaping emissions were collected using a cold trap apparatus on dry ice to condense emission products. One 4 s puff was taken at intervals of 30 s using a 0.4 L min^{-1} air flow rate, which was controlled by a 0.46 L min^{-1} critical orifice connected a diaphragm pump (Gast Manufacturing Inc.) (Figure S2). After 20 puffs, the vape pen was rested for 10-20 minutes to prevent overheating of the battery and cartridge. Collections were repeated a total of 4 times for quantification and statistical analysis.

Condensed vaping emissions were dissolved in ACN for chemical analysis or in cell culture media for cell exposure. To increase the solubility of VEA vaping emissions in aqueous media, DMSO was added to each collection so that the final concentration was 0.1 % v/v DMSO.

2.3 GC/MS Analysis

GC/MS (Agilent 6890N GC and 5975C inert MSD equipped with an electron ionization (EI) ion source) analysis was performed to identify and quantify decomposition products from VEA vaping. The detailed procedures for the operation of GC/MS have been reported previously.[20] For non-polar compounds such as untransformed VEA, 2 μL of samples were directly injected into an Agilent J&W DB-5MS column (30 m × 0.25 mm i.d., 0.25 μm film) for separation. The GC was set to 60 °C for 1 min, ramped to 150 °C at a rate of 3 °C min^{-1}, held at 150 °C for 2 min, ramped to 310 °C at a rate of 20 °C min^{-1}, and held at 310 °C for 5 min. A solvent delay of 6 min was used. For polar degradation products such as DQ, 2 μL of sample were directly injected into a Rtx-VMS fused silica column (30 m × 0.25 mm i.d., 1.4 μm film). The GC was set to 35 °C for 1 min, ramped to 240 °C at a rate of 10 °C min^{-1}, and held 4 min. A solvent delay of 6 minutes was also used. Compounds were identified using the NIST 2008 mass spectral database; emission products were confirmed and quantified using corresponding authentic or surrogate standards dissolved in ACN.

2.4 Cell Culture

Human bronchial epithelial cells (BEAS-2B) were purchased from the American Type Culture Collection (ATCC). Cells were cultured in either Gibco® LHC-9 medium (1X) (Invitrogen) or supplemented Bronchial Epithelial Growth Medium (BEGM; Lonza). Cells were incubated at 37 °C and 5% CO_2 until confluent (75-80%) and transferred to 96- or 24-well plates for exposure experiments.

2.5 Cytotoxicity Analysis

BEAS-2B cells were grown in 96-well plates at initial seeding densities of 6×10^3 cells per well and allowed 24 hours for attachment. Wells were then treated with 2-fold dilutions of VEA vaping emissions, unvaped VEA, or DQ standard for 24 hours. The highest concentration of VEA vaping emissions and unvaped VEA used to expose cells was 125 mg/mL, though the actual concentration available to cells may have been lower due to solubility issues. The highest concentration of DQ used was 25 μg/mL as this was the corresponding concentration of DQ produced in VEA vaping emissions at the time of cell exposure. Untreated cells were included as negative controls, while cells treated with 0.1% v/v Triton X-100 were used as a positive control to simulate 100% cell death. DMSO was added to each treatment so that the final concentration was 0.1 % v/v. To account for cytotoxicity induced by DMSO, 0.1% v/v DMSO in media was used as a vehicle control. Finally, 100 puffs of vaped deionized (DI) water was used as a vaping device control. To measure cytotoxicity after exposure, the lactate dehydrogenase (LDH) cytotoxicity assay was used as a measure of cell membrane integrity. The assay was performed following the manufacturer's protocol (Roche) and absorbance was measured on a TECAN SpectraFluor Plus microplate reader at 490 nm, with a reference wavelength at 620 nm. Light absorbance by the mixture of LDH assay reagent and treatments themselves was also considered and subtracted before analysis.

2.6 Detection of ROS

2.6.1 Acellular 2'-7'-Dichlorodihydrofluorescein ($DCFH_2$) Assay—To measure exogenous ROS production, the $DCFH_2$ fluorescent assay was used. 200 μL of a 5 mM $DCFH_2DA$ solution in DMSO was chemically hydrolyzed with 4.8 mL of 0.01 M NaOH for 30 minutes in the dark. After 30 minutes, 10 mL of 1 X PBS was added to neutralize the reaction and reduce the risk of auto-oxidation[21]; the solution was then placed on ice in the dark until use to prevent photo-oxidation. 100 μL of either dilutions of DQ, unvaped VEA, or VEA vaping emissions in DMSO were added to the wells of a black, clear bottom 96-well plate (Corning), followed by 100 μL of chemically hydrolyzed $DCFH_2$. To account for background fluorescence or photo- or auto-oxidation of $DCFH_2$, $DCFH_2$ in DMSO only (no treatment added) was also assessed. To account for the role of metals in ROS generation, 100 puffs of vaped DI water were used as a vaping device control. Finally, 120 μM of TBHP was used as a positive control to induce ROS production. Fluorescence intensity was measured every 5 minutes for 75 minutes (excitation: 485 nm, emission: 535 nm) using a GloMax Multi+ Plate Reader (Promega) with Instinct® Software.

2.6.2 Cellular $DCFH_2DA$ Assay—The $DCFH_2DA$ assay was also performed in the cellular system to measure intracellular ROS in BEAS-2B cells. Cells were seeded in 96-well plates at densities of 6×10^3 cells per well for 24 hours at 37 °C prior to exposure. After 24 hours, the media was removed, and each well was washed with 50 μL of PBS. After washing, cells were exposed to 100 μL of a 15 μM solution of $DCFH_2DA$ in cell culture media and incubated at 37 °C for 45 minutes. The dye solution was subsequently removed and 100 μL of treatment or control groups were added upon exposure. All treatments in media contained 0.1 % v/v of DMSO. Background fluorescence of cell-free $DCFH_2DA$ in

media with 0.1 % v/v DMSO was also measured. The fluorescence intensity was measured following the same protocol as described in section 2.6.1.

2.7 Biomarker Analysis

2.7.1 Cell Exposure, RNA Extraction and Purification—To assess the alteration of oxidative stress-associated gene expression, BEAS-2B cells were seeded in 24-well plates at densities of 6×10^4 cells per well and allowed 24 hours for attachment. Cells were then exposed to 65 mg mL^{-1} of VEA vaping emissions, 65 mg mL^{-1} of unvaped VEA, 12.5 μg mL^{-1} of DQ standard, 100 puffs of vaped DI water, or 50 μM of TBHP for 6 hours to assess expression of heme oxygenase I (*HMOX-1*) and 24 hours to assess expression of NAD(P)H quinone dehydrogenase 1 (*NQO1*) (Figure S3). Untreated cells were included as negative controls. After exposure, cells were lysed with 300 μL of cold TRI Reagent (Zymo Research) for total RNA isolation. The RNA was extracted using the Direct-zol RNA MiniPrep kit (Zymo Research). A Nanodrop ND-2000C spectrophotometer (Thermo Fisher Scientific) was used to determine the RNA quality (A260/280 ratios) and concentrations. A260/280 ratios for all RNA samples chosen for gene expression analysis were above 1.8. Purified RNA samples were stored at −80 °C until further processing.

2.7.2 qPCR—Expression levels of *NQO1*, and *HMOX-1* genes were measured using the one-step QuantiFast SYBR Green® RT-PCR kit (Qiagen). The QuantiTect Primer Assays (Qiagen) of *NQO1* (GeneGlobe ID: QT00050281) and *HMOX-1* (GeneGlobe ID: QT00092645) were used in this study. The results were normalized to a housekeeping gene beta-actin (*ACTB*) (Qiagen, GeneGlobe ID: QT00095431) and expressed as $\log_2$ fold changes over the unexposed controls. A CFX96 Touch Real Time PCR detection system (Bio-Rad) was used. Thermal cycling conditions for RT-PCR were set as follows: 10 min at 50 °C for reverse transcription, 5 min at 95 °C for initial denaturation and 40 cycles of amplification (10 s at 95 °C and 30 s at 60 °C).

2.8 Aerosol Analysis

A Scanning Electron Mobility Spectrometer (SEMS; Brechtel Manufacturing Inc.) was used to determine the volume and size distribution of VEA vaping aerosols emitted directly from the vape pen. The aerosol collection efficiency of the cold trap method was determined by measuring the volume and number concentrations at the inflow and outflow of a first cold trap, and the outflow of a second cold trap (figure S4).

A micro-orifice uniform deposit impactor (MOUDI, Mo. 110; MSP Corporation) was used to determine the distribution of identified compounds in different sizes of aerosols. To collect size-fractionated aerosol samples, the vape pen was connected to a 4 L jar; emissions were vaped into the jar using the previously described protocol. A diaphragm pump was used to pull emissions through the MOUDI at a flow rate of 30 L min^{-1}. The pump was allowed to run for 1 hour after completion of aerosol generation to ensure that all particles were deposited on MOUDI stages lined with aluminum foil. Collected size-fractionated vaping aerosols on foil stages were extracted with 5 mL of ACN and sonicated for 30 mins. Samples were dried with a gentle N_2 gas stream to 100 μL, with 10 μL of 1, 3, 5-TCB solution (2 μg/μL) added to the samples as an internal standard, and subsequently analyzed

using GC/MS following the method described in section 2.3. The experimental set-up is shown in the SI (Figure S5A).

To verify the cut sizes of MOUDI stages, 0.27 μm green fluorescent microspheres (ThermoFisher Scientific) that correspond to the mode of vaping aerosol size distribution were nebulized and pulled through the MOUDI to deposit on the foil-lined stages. Figure S5B shows the microspheres deposited at the expected cut size, confirming the stages expected to see the majority of VEA vaping emissions.

2.9 Statistical Analysis

GraphPad Prism 9 was used to analyze differences in $DCFH_2DA/DCFH_2$ activities and gene expression levels after treatment. Two-way Analysis of Variance (ANOVA) with Tukey HSD *post-hoc* analysis was used to determine the statistical significance of treatments compared to the untreated control. A p-value < 0.05 was considered statistically significant.

3. Results and Discussion

3.1 GC/MS Analysis of VEA Emissions

Previous studies have found that several factors can impact the formation and collection efficiency of various compounds in vaping emissions, including model of e-cigarette tested, puffing topography (e.g., puff duration, puffing interval, and air flow rate), and collection method.[18, 22, 23] GC/MS analysis of VEA vaping emissions at 3.6 V revealed a wide range of decomposition products (Figure S6 and S7). While a large portion of the spectra remains unidentified, we were able to attribute approximately 21% of the total mass of VEA consumed by the vape pen to major emission products of duroquinone, durohydroquinone (DHQ), vitamin E, and VEA. We have also tentatively identified 3, 7, 11-trimethyl-1-dodecanol as a decomposition product based on a consistent NIST MS spectral library reverse match score of 900 or greater, and 1-pristene based on comparison of experimental mass spectra with spectra previously reported in literature by Mikheev et al.[24], which describes fragment ions of m/z 111, 126, and 181 that are consistent with our results. Due to the lack of available authentic standards, 1-dodecanol was used as a surrogate to quantify 3, 7, 11-trimethyl-1-dodecanol and 1-pristane was used to quantify 1-pristene. Table 1 summarizes the production yields of each identified compound per mg of VEA consumed by the vape pen. Information regarding predicted molecular weight, boiling point, and vapor pressures of compounds was obtained from ChemSpider[25] based on the estimates from Environmental Protection Agency (EPA)'s EPI Suite program. The determined yields were used to calculate the concentrations of DQ standard expected to be found in corresponding vaped VEA collections for use in cell exposures. To account for variations between vaping aerosol collections, production yields of DQ were quantified prior to each cell exposure experiment to determine the corresponding DQ concentrations in each vaped VEA treatment.

The detection of these products is consistent with prior findings,[10, 11, 24] though the mass yield of DQ shown here is 3 times lower than previously reported.[11] This difference may be attributed to an increased flow rate compared to our previous study, which may

decrease the residence time the of parent oil in the cartridge and ultimately decrease the amount of VEA that is transformed by the heated coil. In addition, other studies have identified decomposition products that could not be found in our spectra, such as ketene or durohydroquinone monoacetate (DHQMA).[10, 24] Absence of these compounds in our spectra may be attributed to differences in the collection method and vape pen operation. The cold trap collection method used in this study was optimized for the collection of compounds such as DQ and VEA, whose boiling points are well above the temperature of dry ice and are easily captured for analysis. For compounds with high vapor pressure, such as ketene, the use of dry ice to condense emissions may not capture gas-phase products as efficiently as liquid nitrogen used in prior studies.[10] Ketene, which has an approximate boiling point of −56 °C[25], was not expected to be observed in our collection. In addition, observation of carbonyl-containing compounds from GC/MS often requires derivatization methods that were not used in this study[10, 26]. As such, it is highly likely that ketene and other higher volatility compounds are produced during the vaping process but cannot be observed in our results.

Furthermore, the current study analyzed vaping emissions produced at an average peak temperature of 218 °C (3.6 V), which is a lower temperature than what has previously been reported in literature at similar applied voltages for VEA vaping.[27, 28] Differences in measured coil temperature may be attributed to the design of the device used. In Lynch et al.[27] and Wu et al.[10], where coil temperatures reach up to 600 °C, coils with 0.25 to 1.8 Ω resistance were used, compared to the 2.2 Ω resistance coil at 3.6 V used in our study. This difference in coil resistance may impact the resulting power output and the temperatures the heating element was able to reach, even when operated at the same voltage setting. The cartridge in this study was chosen as it is a product intended for use in THC vaping and was a brand found to be used by patients who developed EVALI symptoms.[7, 29] It is highly possible that the temperature used in VEA vaping may impact the identity and quantity of certain decomposition products.[30].

Finally, previous reports of VEA thermal degradation have found VEA to be thermally stable up to temperatures ≥ 250 °C[31]; in addition, the temperature used here (218 °C) is, to our knowledge, the lowest reported temperature at which DQ production has been observed. The differences in these findings may be attributed to a catalytic effect between VEA oil and the metal constituents of the cartridge that the oil must come into contact with during vaping. One study by Saliba et al.[32] recently investigated the pyrolysis of propylene glycol (PG) and found that the presence of a metal heating coil during pyrolysis greatly impacted the temperature at which PG began to decompose into carbonyl-containing compounds. In the presence of stainless steel, Kanthal, or aged nichrome, the temperature at which peak methylglyoxal production was observed was decreased by nearly 300 °C compared to pure pyrolysis in the absence of metal. Thus, is it highly possible that VEA may be interacting with metals in the device in a similar way, resulting in a catalytic effect to degrade VEA at lower temperatures. However, further study into the impact of temperature and vaping device construction of VEA degradation should be explored.

3.2 Cytotoxicity Analysis

BEAS-2B cells were exposed to 2-fold serial dilutions of unvaped VEA, VEA vaping emissions, and DQ standard for 24 hours before cytotoxicity was assessed. The results of the LDH assay support our prior findings of differential toxicity after the vaping process.[11] There is a considerable shift in cytotoxicity between cells exposed to unvaped VEA and those exposed to VEA vaping emissions (Figure 1); a clear dose-dependent response can likewise be observed when cells are exposed to DQ alone. Neither the vehicle nor device controls demonstrated significant cytotoxicity. At corresponding DQ concentrations, DQ can account for nearly 50% of the observed cytotoxicity in VEA vaping emission-exposed cells. Concentrations not found to be overly toxic (≤ 30%) within the 24-hour exposure period were chosen for further gene expression analysis[33].

3.3 ROS Production

$DCFH_2DA$ is a fluorescent assay used to measure general oxidative potential in both cellular and acellular systems. In its non-fluorescent form, $DCFH_2DA$ can easily enter through lipid membranes.[21, 34] Once transported into the cytosol, it may be deacetylated by intracellular esterases, converting it to $DCFH_2$, a non-fluorescent form that cannot cross cellular membranes as readily and can be oxidized by reactive species to form the fluorescent product 2',7'-dichlorofluorescein (DCF).[21, 34-36] The deacetylation process can also be done in acellular systems by chemically hydrolyzing $DCFH_2DA$ into $DCFH_2$ using NaOH;[35, 37, 38] this form can then be oxidized by a compound of interest and/or generated H_2O_2 (Figure S8).

Quinones such as DQ are highly electrophilic and have the potential to generate large amounts of ROS through redox cycling; generated ROS can then damage cellular membranes and other macromolecules critical to regular function. However, assessment of only this exogenous oxidative potential does not account for ROS generated by the cell itself during metabolic processes or immune responses to a xenobiotic.[39, 40] Endogenous ROS can contribute greatly to intracellular redox homeostasis, further inducing oxidative stress.[41, 42] Assessment of both the oxidative potential and the total cellular ROS produced upon exposure to a toxicant can help to better elucidate the mechanism of toxicity and the risk of oxidative damage to cells.

The $DCFH_2DA/DCFH_2$ assay was studied in both acellular and cellular systems over 75 minutes after either addition of the $DCFH_2$ or exposure of treatments and controls to BEAS-2B. The time course results of both assays can be found in the SI (Figure S9). Figure 2 summarizes the exogenous oxidative potential of treatments in the acellular system (Figure 2A) and the intracellular ROS measured in BEAS-2B exposed to treatments (Figure 2B); results are expressed as the fold change in fluorescence intensity compared to the negative control. After 75 minutes, neither unvaped VEA nor the device control induce significant ROS generation in either system. In the acellular system, DQ and VEA vaping emissions both demonstrate the ability to generate ROS significantly compared to the solvent alone; note that equivalent concentrations of DQ standard alone shows greater ROS production than VEA vaping emissions. In addition, all concentrations of DQ standard reacted more quickly with $DCFH_2$ than VEA vaping emissions (Figure S9B and C). In the cellular

system, however, only the highest concentration of VEA vaping emissions resulted in significant ROS generation ($p = 0.0329$).

In the acellular system, DQ was expected to demonstrate high $DCFH_2$ oxidation both through the generation of ROS during redox cycling, as well as through direct oxidation by DQ or adduct formation of DQ and $DCFH_2$ via Michael addition. While DQ is an electrophilic compound and has already been observed in the vaping emissions, VEA emissions constitute a mixture of electrophiles, metals, and antioxidants (such as vitamin E) that may compete with the $DCFH_2$ probe to be oxidized. These nontarget interactions may suppress the overall response observed by VEA vaping emissions compared to DQ alone in the acellular system. In the cellular system, there exists an even larger array of scavengers – biomolecules, lipids, and other antioxidants – that may compete with the probe to be oxidized by generated ROS. Antioxidant molecules may also interact with the probe itself and cause attenuation of the probe before it is able to be oxidized by ROS,[43] resulting in a reduced signal compared to the acellular system. For DQ-treated cells, it is likely that the concentration of DQ is not great enough to overcome competition by scavengers, resulting in decreased ROS production or ability to stimulate endogenous ROS production. In contrast, the highest concentration of VEA vaping emissions, being a mixture of degradation products, may have contained a greater amount of electrophilic species to compete with scavengers to oxidize $DCFH_2$, and/or contained compounds able to induce endogenous ROS production by the cells.[41] Nevertheless, these findings support that VEA vaping emissions and DQ are both capable of generating ROS that may induce oxidative damage in exposed cells.

3.4 Gene Expression Analysis

The relative levels of gene expression for the exposure and control groups, expressed as the $\log_2$ fold changes, were calculated using the comparative cycle threshold ($2^{-\Delta\Delta CT}$) method.[44] *NQO1* was chosen as a biomarker of quinone toxicity as the enzyme is known to compete with quinone reduction pathways that may initiate quinone redox-cycling;[45] DQ has been used in several studies as model quinone substrate to induce *NQO1* expression in various cell types.[46-48] *HMOX-1*, in contrast, is a stress-induced enzyme and is a commonly used biomarker of downstream oxidative damage.[49] Our results show that exposure to DQ and VEA vaping emissions results in significant upregulation of *HMOX-1* and *NQO1* compared to the untreated control (Figure 3). *HMOX-1* and *NQO1* expression by vaping emissions was found to be significantly greater than expression seen in DQ-exposed cells ($p < 0.0001$ for *HMOX-1* expression and $p = 0.0391$ for *NQO1* expression). Neither unvaped VEA, the DMSO vehicle control, nor the water device control resulted in significant gene expression change of either biomarker.

NQO1 and *HMOX-1* upregulation by DQ and VEA vaping emissions provides evidence that quinones are present in vaping emissions at concentrations that pose a risk to the alteration of cellular homeostasis, and that both DQ alone and VEA vaping emissions have the potential to induce oxidative damage through the production of ROS or reactions with biomolecules to disrupt redox signaling pathways[50, 51]. The ability of VEA vaping emissions to both induce greater *NQO1* and *HMOX-1* expression than DQ standard alone,

highly suggests that VEA vaping emissions may contain a mixture of electrophiles and ROS inducers that are capable of inducing oxidative damage. The significant difference in *NQO1* expression between DQ and vaping emissions may imply the presence of more quinones and quinone-containing species than DQ alone. In addition, studies have found that oxidation of vitamin E by free radicals or ROS results in the generation of vitamin E quinone, which can be reduced by *NQO1* to a hydroquinone and again act as an antioxidant.[52] Thus, the increased upregulation of both *NQO1* and *HMOX-1* may also be attributed to interactions between VEA decomposition products in the total mixture. These results overall support that quinone toxicity is one contributing mechanism through which the VEA vaping-induced lung oxidative damage occurs, but the presence of other degradation compounds and metals from the device may either enhance DQ toxicity or provide additional mechanisms of toxicity.

3.5 Aerosol Analysis

The majority of particles emitted directly from the vape pen existed between 200 to 400 nm in diameter, though a small fraction of particles can be observed between 60 to 100 nm (Figure 4A and B). This observed size distribution agrees with recent studies of aerosolized VEA at approximately the flow rate used.[11, 24] The total aerosol collection efficiency of our collection method was estimated to be ≥ 99.9% by both volume and number (Figure 2B and C) after tandem cold trap collection.

Size of emitted particles will greatly impact lung deposition, with smaller particles (≤ 100 nm) capable of penetrating into the lower conducting airways and the alveolar region of the lungs.[53, 54] Based on these results, VEA vaping emissions overall have the potential to penetrate into the lower respiratory system of vape users. To determine the sizes at which DQ and other identified compounds are enriched that have direct implications for the associated risk of lung deposition, we analyzed size-fractionated aerosol composition in vaping emissions. Table 2 depicts the mass fractions of the major decomposition products found from chemical analysis. The stages containing the largest total mass of particles deposited were those with cut sizes ranging between 180 to 1000 nm. We observed that VEA could be found at all sizes, while the first major decomposition product, vitamin E, favored particle sizes above 180 nm, but was not detectable above 1000 nm. 3, 7, 11-trimethyl-1-dodecanol showed the greatest fraction in the larger sized particles (560 nm and above) but was found at detectable levels in particles smaller than 100 nm. DHQ was detectable at diameters greater than 180 nm, but only showed substantial deposition above 560 nm. This contrasts with DQ, which could only be found at sizes below 560 nm. The greatest mass fraction of DQ was observed in particles 56 to 100 nm in diameter. 1-Pristene was not detectable at any particle size. The inability to detect 1-pristene is likely attributable to fast oxidation of the double bond by ozone from room air, which was present at background levels between 30-40 ppbv.[55, 56] This background concentration of ozone was not expected to substantially influence the detection of the other target compounds.

Ultimately, VEA, 3,7,11-Trimethyl-1-docecanol, DQ were observed to exist as particles with diameters less than 100 nm and therefore are likely the main products able to penetrate the alveolar region of the lungs. The decomposition products show clear potential for

differential lung deposition in those who vaped VEA. One recent study found that the chemical composition of e-cigarette aerosols are size dependent and heavily dependent on boiling point and vapor pressure of the aerosol constituents.[57] As shown in Table 1, the vapor pressures of emitted products vary greatly, which in turn may impact their gas-particle partitioning behavior once released into the environment. This compositional difference in particle size may impact the risk of exposure and negative health effects to people in proximity to active vapers (i.e., passive vaping). With the exception of 1-pristene, transformation of aerosols, or aging, after vaping was not expected to substantially influence the results due to the short residence time in the jar and hydrophobic nature of the target compounds. It is possible that some more hygroscopic constituents may absorb water vapor from room air if left over time.[58] This process could drastically impact the size of particles, resulting in larger particles that are more likely to deposit in different regions of the airways when inhaled by bystanders. However, to fully understand the dynamic nature of these particles in the environment and the exposure risk via passive vaping, further study is required.

3.6 Potential Limitations

Some further limitations to this study should be noted. First, VEA was studied individually in an isolated system to examine the formation and contribution of DQ to oxidative lung injuries, while cartridges linked to EVALI cases were often blends with varying ratios of VEA and THC. A prior study reported that in both liquid and aerosol phases, THC and VEA can form hydrogen bonded complexes.[59] In addition, a study by Muthumalage et al[60] recently found that exposure of BEAS-2B cells and mice to CBD/counterfeit cartridges resulted in greater ROS generation and inflammatory responses than VEA alone. The role of the interactions between these complexes in VEA-induced lung toxicity has not been investigated at this time. Furthermore, the toxicological responses following exposure were studied using an immortalized, monoculture cell line, which does not allow for investigation into the systemic effects *in vivo*. While the parent VEA molecule was not found to induce cytotoxicity in our study, recent reports have demonstrated that VEA and other e-liquids may interact with pulmonary surfactant at the air-liquid interface, resulting in mechanical injury to the lungs that may contribute to EVALI-symptom onset.[61, 62] Finally, decomposition product formation was investigated at one voltage/temperature setting and puffing topography. However, vaping behavior may vary drastically between users, which has been found to alter composition,[18, 63] and size and volume distributions[22, 24] of aerosols. The vaping topography used in this study was adapted from previous literature on nicotine vaping, but less is known about the parameters used in THC-vaping.[64] As a result, those who vaped VEA could have been exposed to differing concentrations of DQ or aerosol compositions than observed in this study.

4. Conclusions

This study investigated the potential contribution of the thermal decomposition product DQ in VEA vaping emissions to induce oxidative stress in exposed lung cells. Our results show that DQ and VEA vaping emissions show significant potential to generate ROS, potentially causing oxidative damage to biomolecules. Moreover, VEA vaping emissions

were found to be linked to the upregulation of *NQO1* (a quinone-metabolizing enzyme) and *HMOX-1* (an oxidative stress biomarker) genes, providing evidence of vaping-induced oxidative stress and quinone toxicity as one potential mechanism. Finally, our results support that decomposition products of VEA may deposit at different lung depths. DQ in particular was found to exist at sizes below 100 nm, suggesting its potential to penetrate into the alveolar region of the lungs. Notably, the differential responses between DQ- and VEA vaping emission-exposed cells highlight the need to further investigate the decomposition products of VEA during vaping. The increased responses induced by VEA vaping emissions suggest that while quinone toxicity has a high potential to damage cells, it is likely that the vaping emissions contain a mixture of electrophilic compounds (e.g., aldehydes or ketones), ROS inducers, and metal catalysts that may enhance VEA's oxidative potential. In essence, while our results provide evidence that quinone toxicity may be one of the molecular mechanisms through which VEA vaping causes oxidative lung injuries, it may be one of several mechanisms. It is likely that EVALI symptoms may be the result of synergistic interactions between DQ and other vaping emission products from VEA and THC[60]. To fully understand the molecular mechanisms through which VEA vaping causes lung injury, future studies are required to investigate the potential interactions between decomposition products. The wide variability in the chemical compositions that users may have been exposed to as a result of variations in vaping behavior must also be explored in future works.

Supplementary Material

Refer to Web version on PubMed Central for supplementary material.

Acknowledgments

This work was supported by the UCR Regents Faculty Development Award awarded to Ying-Hsuan Lin. Alexa Canchola was supported by an NRSA T32 training grant (T32 ES18827). We would like to thank the UCR Genomics Core Facility for the use of their instrumentation. We also thank Dr. Roya Bahreini and Dr. Prue Talbot at UCR for the use of the micro-orifice uniform deposit impactor (MOUDI) and for their valuable comments on the analysis of the reported results.

ABBREVIATIONS

EVALI	e-cigarette or vaping associated lung injury
VEA	vitamin E acetate
DQ	duroquinone
DHQ	durohydroquinone

References

(1). Miech R, Johnston L, O'Malley PM, Bachman JG, and Patrick ME (2019) Adolescent Vaping and Nicotine Use in 2017–2018 — U.S. National Estimates. New England Journal of Medicine 380, 192–193.

(2). McKeganey N, Barnard M, and Russell C (2018) Vapers and vaping: E-cigarettes users views of vaping and smoking. Drugs: Education, Prevention and Policy 25, 13–20.

(3). CDC. (2020) Outbreak of Lung Injury Associated with the Use of E-Cigarette, or Vaping, Products, CDC Online Newsroom.

(4). Lozier MJ, Wallace B, Anderson K, Ellington S, Jones CM, Rose D, Baldwin G, King BA, Briss P, and Mikosz CA (2019) Update: demographic, product, and substance-use characteristics of hospitalized patients in a nationwide outbreak of e-cigarette, or vaping, product use–associated lung injuries—United States, December 2019. MMWR Morb Mortal Wkly 68, 1142.

(5). Layden JE, Ghinai I, Pray I, Kimball A, Layer M, Tenforde M, Navon L, Hoots B, Salvatore PP, and Elderbrook M (2019) Pulmonary illness related to e-cigarette use in Illinois and Wisconsin—preliminary report. New England Journal of Medicine.

(6). Blount BC, Karwowski MP, Shields PG, Morel-Espinosa M, Valentin-Blasini L, Gardner M, Braselton M, Brosius CR, Caron KT, Chambers D, Corstvet J, Cowan E, De Jesüs VR, Espinosa P, Fernandez C, Holder C, Kuklenyik Z, Kusovschi JD, Newman C, Reis GB, Rees J, Reese C, Silva L, Seyler T, Song M-A, Sosnoff C, Spitzer CR, Tevis D, Wang L, Watson C, Wewers MD, Xia B, Heitkemper DT, Ghinai I, Layden J, Briss P, King BA, Delaney LJ, Jones CM, Baldwin GT, Patel A, Meaney-Delman D, Rose D, Krishnasamy V, Barr JR, Thomas J, and Pirkle JL (2020) Vitamin E Acetate in Bronchoalveolar-Lavage Fluid Associated with EVALI. New England Journal of Medicine 382, 697–705.

(7). Duffy B, Li L, Lu S, Durocher L, Dittmar M, Delaney-Baldwin E, Panawennage D, LeMaster D, Navarette K, and Spink D (2020) Analysis of Cannabinoid-Containing Fluids in Illicit Vaping Cartridges Recovered from Pulmonary Injury Patients: Identification of Vitamin E Acetate as a Major Diluent. Toxics 8.

(8). Berton TR, Conti CJ, Mitchell DL, Aldaz CM, Lubet RA, and Fischer SM (1998) The effect of vitamin E acetate on ultraviolet-induced mouse skin carcinogenesis. Molecular Carcinogenesis 23, 175–184. [PubMed: 9833778]

(9). Ogunwale MA, Li M, Ramakrishnam Raju MV, Chen Y, Nantz MH, Conklin DJ, and Fu X-A (2017) Aldehyde Detection in Electronic Cigarette Aerosols. ACS Omega 2, 1207–1214. [PubMed: 28393137]

(10). Wu D, and O'Shea DF (2020) Potential for release of pulmonary toxic ketene from vaping pyrolysis of vitamin E acetate. PNAS 117, 6349–6355. [PubMed: 32156732]

(11). Jiang H, Ahmed CMS, Martin TJ, Canchola A, Oswald IWH, Garcia JA, Chen JY, Koby KA, Buchanan AJ, Zhao Z, Zhang H, Chen K, and Lin Y-H (2020) Chemical and Toxicological Characterization of Vaping Emission Products from Commonly Used Vape Juice Diluents. Chem. Res. Toxicol 33, 2157–2163. [PubMed: 32618192]

(12). Ross D, and Siegel D (2018) NQO1 in protection against oxidative stress. Current Opinion in Toxicology 7, 67–72.

(13). Attia SM (2010) Deleterious Effects of Reactive Metabolites. Oxidative Medicine and Cellular Longevity 3, 948013.

(14). Bolton JL, Trush MA, Penning TM, Dryhurst G, and Monks TJ (2000) Role of quinones in toxicology. Chem. Res. Toxicol 13, 135–160. [PubMed: 10725110]

(15). O'Brien PJ (1991) Molecular mechanisms of quinone cytotoxicity. Chem. Biol. Interact. 80, 1–41. [PubMed: 1913977]

(16). Shang Y, Zhang L, Jiang Y, Li Y, and Lu P (2014) Airborne quinones induce cytotoxicity and DNA damage in human lung epithelial A549 cells: The role of reactive oxygen species. Chemosphere 100, 42–49. [PubMed: 24480427]

(17). Li N, Venkatesan MI, Miguel A, Kaplan R, Gujuluva C, Alam J, and Nel A (2000) Induction of Heme Oxygenase-1 Expression in Macrophages by Diesel Exhaust Particle Chemicals and Quinones via the Antioxidant-Responsive Element. The Journal of Immunology 165, 3393–3401. [PubMed: 10975858]

(18). Williams M, Li J, and Talbot P (2019) Effects of Model, Method of Collection, and Topography on Chemical Elements and Metals in the Aerosol of Tank-Style Electronic Cigarettes. Scientific Reports 9, 13969. [PubMed: 31562360]

(19). Chen W, Wang P, Ito K, Fowles J, Shusterman D, Jaques PA, and Kumagai K (2018) Measurement of heating coil temperature for e-cigarettes with a "top-coil" clearomizer. PLOS ONE 13, e0195925. [PubMed: 29672571]

(20). Chen JY, Jiang H, Chen SJ, Cullen C, Ahmed CMS, and Lin Y-H (2019) Characterization of electrophilicity and oxidative potential of atmospheric carbonyls. Environ. Sci.: Processes Impacts 21, 856–866.

(21). Chen X, Zhong Z, Xu Z, Chen L, and Wang Y (2010) 2′, 7′ -Dichlorodihydrofluorescein as a fluorescent probe for reactive oxygen species measurement: Forty years of application and controversy. Free Radical Research 44, 587–604. [PubMed: 20370560]

(22). Son Y, Mainelis G, Delnevo C, Wackowski OA, Schwander S, and Meng Q (2020) Investigating E-Cigarette Particle Emissions and Human Airway Depositions under Various E-Cigarette-Use Conditions. Chem. Res. Toxicol 33, 343–352. [PubMed: 31804072]

(23). Son Y, Mishin V, Laskin JD, Mainelis G, Wackowski OA, Delnevo C, Schwander S, Khlystov A, Samburova V, and Meng Q (2019) Hydroxyl Radicals in E-Cigarette Vapor and E-Vapor Oxidative Potentials under Different Vaping Patterns. Chem. Res. Toxicol 32, 1087–1095. [PubMed: 30977360]

(24). Mikheev VB, Klupinski TP, Ivanov A, Lucas EA, Strozier ED, and Fix C (2020) Particle size distribution and chemical composition of aerosolized vitamin E acetate. Aerosol Science and Technology 54, 993–998. [PubMed: 33132476]

(25). Pence HE, and Williams A (2010) ChemSpider: An Online Chemical Information Resource. Journal of Chemical Education 87, 1123–1124.

(26). Chen JY, Canchola A, and Lin Y-H (2021) Carbonyl Composition and Electrophilicity in Vaping Emissions of Flavored and Unflavored E-Liquids. Toxics 9.

(27). Lynch J, Lorenz L, Brueggemeyer JL, Lanzarotta A, Falconer TM, and Wilson RA (2021) Simultaneous Temperature Measurements and Aerosol Collection During Vaping for the Analysis of Δ(9)-Tetrahydrocannabinol and Vitamin E Acetate Mixtures in Ceramic Coil Style Cartridges. Front Chem 9, 734793–734793. [PubMed: 34434923]

(28). Zhao T, Shu S, Guo Q, and Zhu Y (2016) Effects of design parameters and puff topography on heating coil temperature and mainstream aerosols in electronic cigarettes. Atmospheric Environment 134, 61–69.

(29). Wagner J, Chen W, and Vrdoljak G (2020) Vaping cartridge heating element compositions and evidence of high temperatures. PLOS ONE 15, e0240613. [PubMed: 33075091]

(30). Geiss O, Bianchi I, and Barrero-Moreno J (2016) Correlation of volatile carbonyl yields emitted by e-cigarettes with the temperature of the heating coil and the perceived sensorial quality of the generated vapours. International Journal of Hygiene and Environmental Health 219, 268–277. [PubMed: 26847410]

(31). Ushikusa T, Maruyama T, and Niiya I (1991) Pyrolysis Behavior and Thermostability of Tocopherols. Journal of Japan Oil Chemists' Society 40, 1073–1079.

(32). Saliba NA, El Hellani A, Honein E, Salman R, Talih S, Zeaiter J, and Shihadeh A (2018) Surface chemistry of electronic cigarette electrical heating coils: Effects of metal type on propylene glycol thermal decomposition. Journal of Analytical and Applied Pyrolysis 134, 520–525. [PubMed: 30906089]

(33). Iso. (2009) Biological evaluation of medical devices—Part 5: Tests for in vitro cytotoxicity. IOS, Switzerland.

(34). LeBel CP, Ischiropoulos H, and Bondy SC (1992) Evaluation of the probe 2', 7'-dichlorofluorescin as an indicator of reactive oxygen species formation and oxidative stress. Chem. Res. Toxicol 5, 227–231. [PubMed: 1322737]

(35). Aranda A, Sequedo L, Tolosa L, Quintas G, Burello E, Castell JV, and Gombau L (2013) Dichloro-dihydro-fluorescein diacetate (DCFH-DA) assay: A quantitative method for oxidative stress assessment of nanoparticle-treated cells. Toxicology in Vitro 27, 954–963. [PubMed: 23357416]

(36). Wang H, and Joseph JA (1999) Quantifying cellular oxidative stress by dichlorofluorescein assay using microplate reader. Free Radical Biology and Medicine 27, 612–616. [PubMed: 10490282]

(37). Huang W, Zhang Y, Zhang Y, Fang D, and Schauer JJ (2016) Optimization of the Measurement of Particle-Bound Reactive Oxygen Species with 2′ ,7′ -dichlorofluorescin (DCFH). Water Air Soil Pollut 227, 164.

(38). Reiniers MJ, van Golen RF, Bonnet S, Broekgaarden M, van Gulik TM, Egmond MR, and Heger M (2017) Preparation and Practical Applications of 2′,7′-Dichlorodihydrofluorescein in Redox Assays. Anal Chem 89, 3853–3857. [PubMed: 28224799]

(39). Klotz L-O, and Steinbrenner H (2017) Cellular adaptation to xenobiotics: Interplay between xenosensors, reactive oxygen species and FOXO transcription factors. Redox Biology 13, 646–654. [PubMed: 28818793]

(40). Sarniak A, Lipińska J, Tytman K, and Lipińska S (2016) Endogenous mechanisms of reactive oxygen species (ROS) generation. Postepy Hig Med Dosw (Online) 70, 1150–1165. [PubMed: 27892899]

(41). Banerjee S, Ghosh J, and Sil PC (2016) Drug metabolism and oxidative stress: cellular mechanism and new therapeutic insights. Biochemistry & Analytical Biochemistry 5, 2161–1009.

(42). Brubacher JL, and Bols NC (2001) Chemically de-acetylated 2′,7′-dichlorodihydrofluorescein diacetate as a probe of respiratory burst activity in mononuclear phagocytes. Journal of Immunological Methods 251, 81–91. [PubMed: 11292484]

(43). Erard M, Dupré-Crochet S, and Nüße OA-O (2018) Biosensors for spatiotemporal detection of reactive oxygen species in cells and tissues. American Journal of Physiology-Regulatory, Integrative and Comparative Physiology 314, R667–R683.

(44). Livak KJ, and Schmittgen TD (2001) Analysis of relative gene expression data using real-time quantitative PCR and the $2^{-\Delta\Delta CT}$ Method. Methods 25, 402–408. [PubMed: 11846609]

(45). Tan AS, and Berridge MV (2010) Evidence for NAD(P)H:quinone oxidoreductase 1 (NQO1)-mediated quinone-dependent redox cycling via plasma membrane electron transport: A sensitive cellular assay for NQO1. Free Radical Biology and Medicine 48, 421–429. [PubMed: 19932748]

(46). Merker MP, Bongard RD, Krenz GS, Zhao H, Fernandes VS, Kalyanaraman B, Hogg N, and Audi SH (2004) Impact of pulmonary arterial endothelial cells on duroquinone redox status. Free Radical Biology and Medicine 37, 86–103. [PubMed: 15183197]

(47). Audi SH, Bongard Rd Fau - Dawson CA, Dawson Ca Fau - Siegel D, Siegel D Fau - Roerig DL, Roerig Dl Fau - Merker MP, and Merker MP (2003) Duroquinone reduction during passage through the pulmonary circulation. American Journal of Physiology-Lung Cellular and Molecular Physiology 285, L1116–L1131. [PubMed: 12882764]

(48). Bianchet MA, Faig M, and Amzel LM (2004) Structure and Mechanism of NAD[P]H:Quinone Acceptor Oxidoreductases (NQO), In Methods in Enzymology pp 144–174, Academic Press.

(49). Gozzelino R, Jeney V, and Soares MP (2010) Mechanisms of Cell Protection by Heme Oxygenase-1. Annual Review of Pharmacology and Toxicology 50, 323–354.

(50). Kansanen E, Jyrkkänen H-K, and Levonen A-L (2012) Activation of stress signaling pathways by electrophilic oxidized and nitrated lipids. Free Radical Biology and Medicine 52, 973–982. [PubMed: 22198184]

(51). Escobar Y-NH, Nipp G, Cui T, Petters SS, Surratt JD, and Jaspers I (2020) In Vitro Toxicity and Chemical Characterization of Aerosol Derived from Electronic Cigarette Humectants Using a Newly Developed Exposure System. Chem. Res. Toxicol 33, 1677–1688. [PubMed: 32223225]

(52). Ross D, and Siegel D (2017) Functions of NQO1 in Cellular Protection and CoQ10 Metabolism and its Potential Role as a Redox Sensitive Molecular Switch. Front. Physiol 8.

(53). Carvalho TC, Peters JI, and Williams RO (2011) Influence of particle size on regional lung deposition – What evidence is there? International Journal of Pharmaceutics 406, 1–10. [PubMed: 21232585]

(54). Lippmann M, Yeates DB, and Albert RE (1980) Deposition, retention, and clearance of inhaled particles. British Journal of Industrial Medicine 37, 337. [PubMed: 7004477]

(55). Grosjean E, and Grosjean D (1997) The Gas Phase Reaction of Unsaturated Oxygenates with Ozone: Carbonyl Products and Comparison with the Alkene-Ozone Reaction. Journal of Atmospheric Chemistry 27, 271–289.

(56). Weschler CJ (2000) Ozone in indoor environments: concentration and chemistry. Indoor air 10, 269–288. [PubMed: 11089331]

(57). Su W-C, Lin Y-H, Wong S-W, Chen JY, Lee J, and Buu A (2021) Estimation of the dose of electronic cigarette chemicals deposited in human airways through passive vaping. Journal of Exposure Science & Environmental Epidemiology 31, 1008–1016. [PubMed: 34239037]

(58). Ranpara A, Stefaniak AB, Williams K, Fernandez E, and LeBouf RF (2021) Modeled Respiratory Tract Deposition of Aerosolized Oil Diluents Used in Δ(9)-THC-Based Electronic Cigarette Liquid Products. Front Public Health 9, 744166–744166. [PubMed: 34805068]

(59). Lanzarotta A, Falconer TM, Flurer R, and Wilson RA (2020) Hydrogen Bonding between Tetrahydrocannabinol and Vitamin E Acetate in Unvaped, Aerosolized, and Condensed Aerosol e-Liquids. Anal Chem 92, 2374–2378. [PubMed: 31951379]

(60). Muthumalage T, Lucas JH, Wang Q, Lamb T, McGraw MD, and Rahman I (2020) Pulmonary Toxicity and Inflammatory Response of Vape Cartridges Containing Medium-Chain Triglycerides Oil and Vitamin E Acetate: Implications in the Pathogenesis of EVALI. Toxics 8.

(61). DiPasquale M, Gbadamosi O, Nguyen MHL, Castillo SR, Rickeard BW, Kelley EG, Nagao M, and Marquardt D (2020) A Mechanical Mechanism for Vitamin E Acetate in E-cigarette/ Vaping-Associated Lung Injury. Chem. Res. Toxicol.

(62). Hayeck N, Zoghzoghi C, Karam E, Salman R, Karaoghlanian N, Shihadeh A, Eissenberg T, Zein El Dine S, and Saliba NA (2021) Carrier Solvents of Electronic Nicotine Delivery Systems Alter Pulmonary Surfactant. Chem. Res. Toxicol 34, 1572–1577. [PubMed: 33945261]

(63). Li Y, Burns AE, Tran LN, Abellar KA, Poindexter M, Li X, Madl AK, Pinkerton KE, and Nguyen TB (2021) Impact of e-Liquid Composition, Coil Temperature, and Puff Topography on the Aerosol Chemistry of Electronic Cigarettes. Chem. Res. Toxicol 34, 1640–1654. [PubMed: 33949191]

(64). Braymiller JL, Barrington-Trimis JL, Leventhal AM, Islam T, Kechter A, Krueger EA, Cho J, Lanza I, Unger JB, and McConnell R (2020) Assessment of Nicotine and Cannabis Vaping and Respiratory Symptoms in Young Adults. JAMA Network Open 3, e2030189. [PubMed: 33351085]

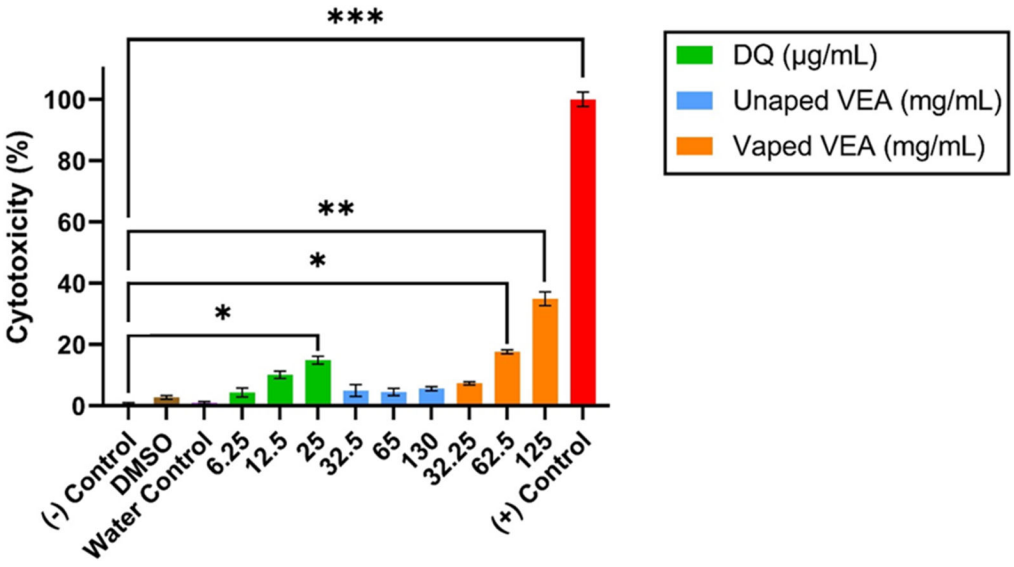

Figure 1.

Cytotoxicity measured by the LDH assay for BEAS-2B cells exposed to unvaped VEA, VEA vaping emissions and DQ standard at corresponding concentrations based on determined production yields. The results are expressed as the mean of three technical replicates (n=3) ± the standard error of the mean (SEM). * indicates $p < 0.05$; ** indicates $p < 0.01$; *** indicates $p < 0.001$.

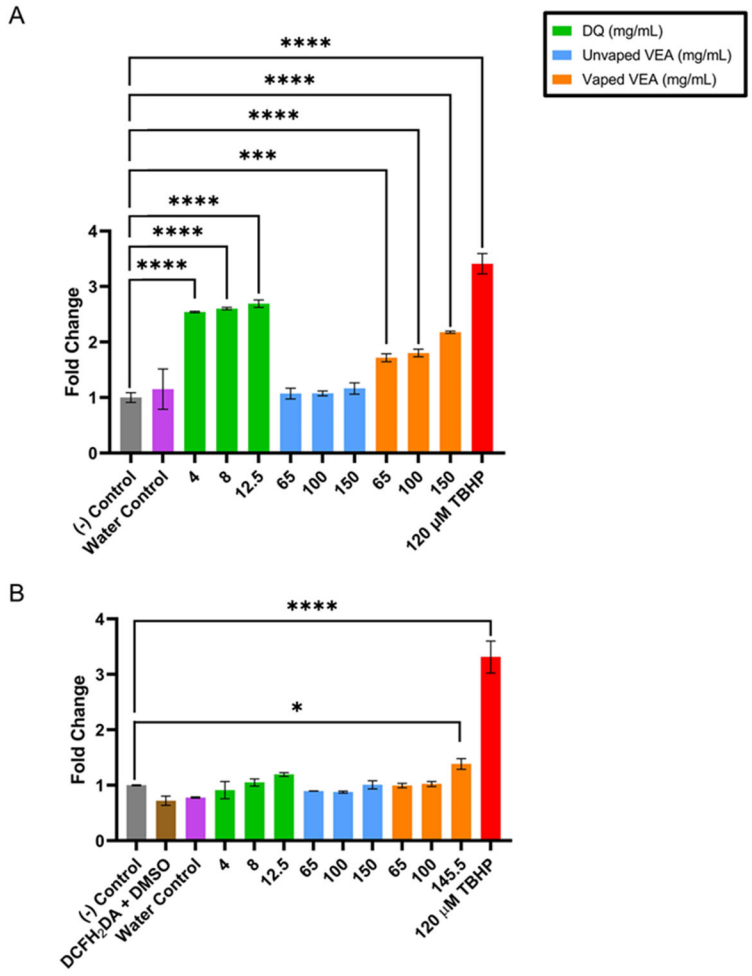

Figure 2.

ROS generated at 75 minutes by unvaped VEA, VEA vaping emissions, DQ standard, and DMSO, water and TBHP positive controls in (A) acellular and (B) cellular systems. Results were normalized to their cytotoxicity and are expressed as fold change in fluorescence intensity over the untreated control in the acellular or cellular system. Each treatment is expressed as the mean ± SEM (n=3) for both acellular and cellular assays. Two-way ANOVA was used to determine statistical significance compared to the negative control. * indicates $p < 0.05$; *** indicates $p < 0.001$; **** indicates $p < 0.0001$.

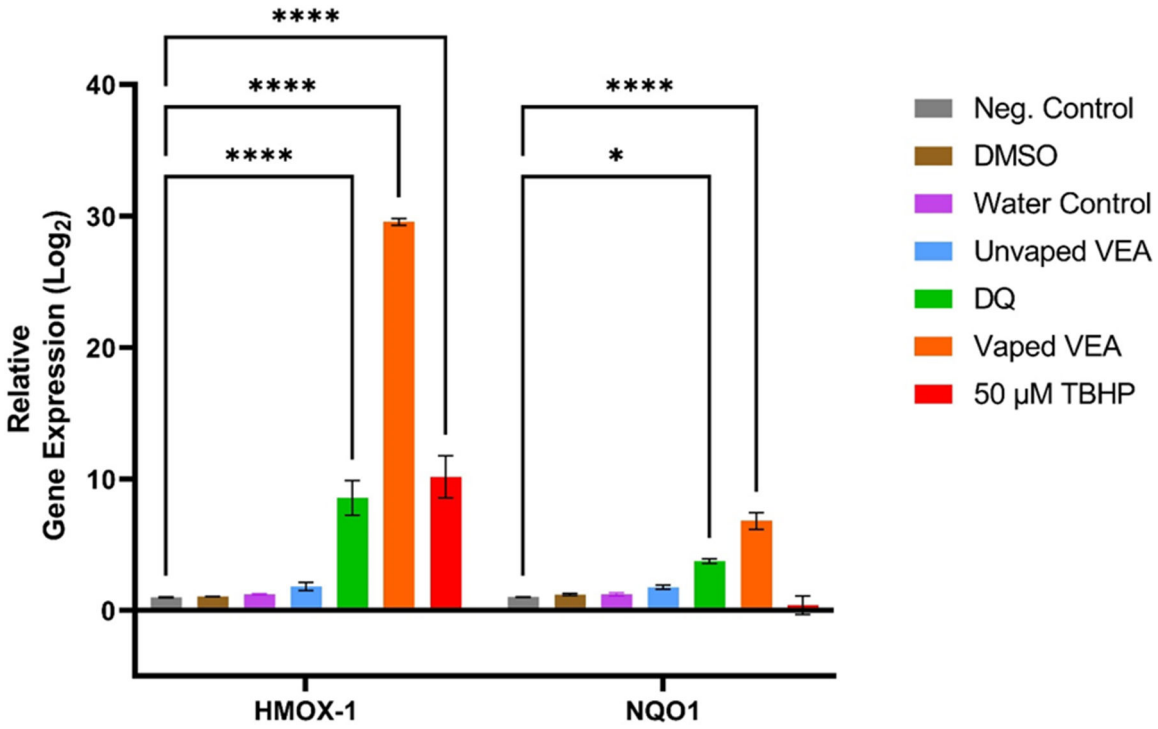

Figure 3.

Relative expression in BEAS-2B cells of *HMOX-1* and *NQO1*genes after 6- and 24-hour exposure, respectively, to 65 mg/mL of VEA vaping emissions, 65 mg/mL of unvaped VEA oil, 12.5 µg/mL of DQ standard, and 100 puffs of vaped DI water collected in cell culture media. 50 µM TBHP was used as a positive control for *HMOX-1* expression. Results are expressed as the mean fold change (log_2) over unexposed controls and normalized to a housekeeping gene (ACTB) ± SEM of 3 samples per treatment (n=3). Two-way ANOVA was used to determine statistical significance compared to the negative control. * indicates $p<0.05$; **** indicates $p<0.0001$.

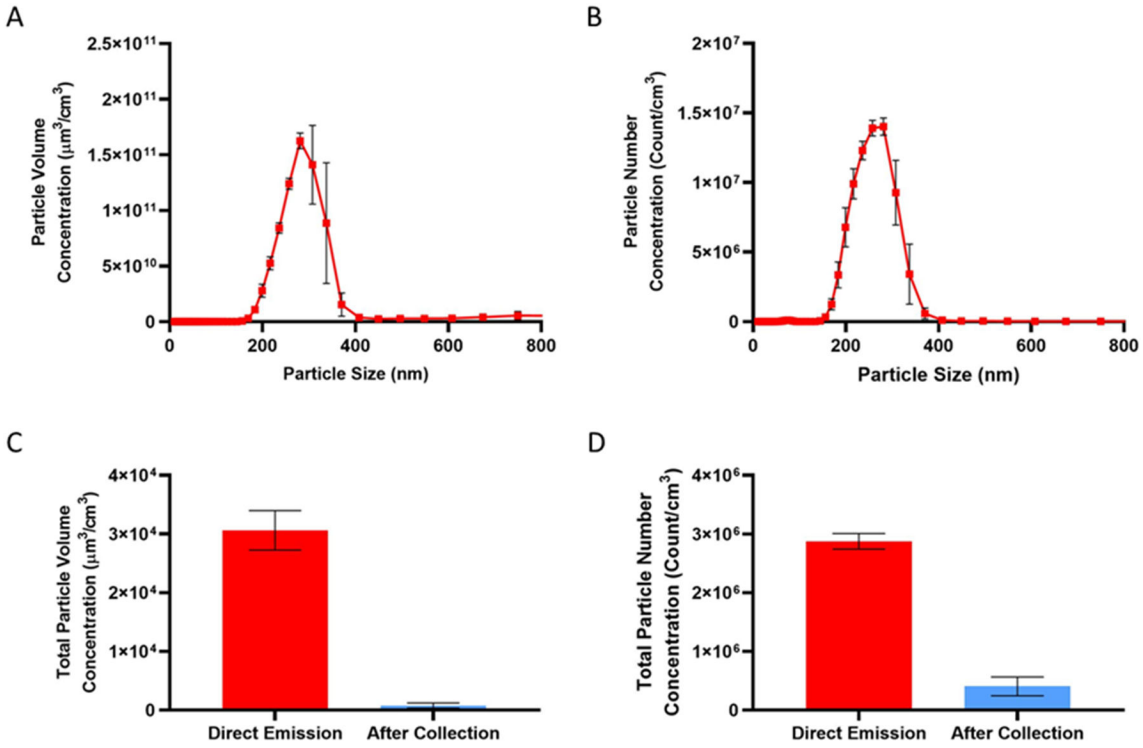

Figure 4.

Size distribution of VEA vaping aerosols characterized by (A) volume and (B) number concentrations. Collection efficiency was determined by comparing the (C) total particle volume concentration and (D) total particle number concentration sampled immediately after emission from the vape pen and after tandem cold trap collection. Particle collection efficiency was estimated to be ≥ 99.9% by both volume and by number. One puff was taken for each SEMS sampling cycle (3 min). Results are expressed as the average of 3 cycles (n=3) after background subtraction.

Table 1.

Summary of VEA vaping emission production yields.

Name	Formula	M.W.[a]	B.P.[b]	Estimated vapor pressure[c]	Structure	EIC (*m/z*)[d]	Production Yield[e]
Vitamin E acetate(VEA)	$C_{31}H_{52}O_3$	472.7	485	4.03×10^{-8}	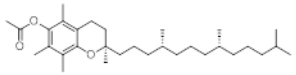	472	$(1.68 \pm 0.09) \times 10^{-1}$
Vitamin E	$C_{29}H_{50}O_2$	430.7	486	1.35×10^{-8}	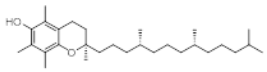	205	$(2.21 \pm 0.01) \times 10^{-2}$
1-Pristene	$C_{19}H_{38}$	266.5	290	5.8×10^{-3}	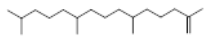	126	$(1.07 \pm 0.07) \times 10^{-2}$
3,7,11-Trimethyl-1-dodecanol	$C_{15}H_{32}O$	228.4	279	2.11×10^{-4}	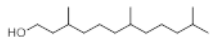	111	$(3.44 \pm 0.20) \times 10^{-4}$
Durohydroquinone (DHQ)	$C_{10}H_{14}O_2$	166.2	312	1.77×10^{-6}	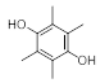	166	$(2.20 \pm 0.13) \times 10^{-4}$
Duroquinone (DQ)	$C_{10}H_{12}O_2$	164.2	230	1.26×10^{-3}		121	$(7.70 \pm 0.28) \times 10^{-5}$

[a] M.W.: molecular weight (g mol^{-1})

[b] B.P.: boiling point (°C) at 1 atm

[c] Estimated vapor pressure: mmHg at 25 °C

[d] Extracted ion chromatogram (EIC); ion selected for quantification

[e] mg-Product recovered mg-VEA comsumed^{-1}

[f] Six major emission products were quantified using authentic or surrogate standards.

Table 2.

Summary of size-fractioned VEA vaping aerosols. Results are expressed as the mass fraction of total mass collected on each MOUDI stage.

Compound name	Mass Fraction						
	d ≤ 56 (nm)	**56 ≤ d ≤ 100 (nm)**	**100 ≤ d ≤ 180 (nm)**	**180 ≤ d ≤ 320 (nm)**	**320 ≤ d ≤ 560 (nm)**	**560 ≤ d ≤ 1000 (nm)**	**1000 ≤ d ≤ 1800 (nm)**
Vitamin E acetate	9.98×10^{-1}	9.51×10^{-1}	9.99×10^{-1}	9.62×10^{-1}	9.60×10^{-1}	9.45×10^{-1}	9.93×10^{-1}
Vitamin E	b.d.l.[a]	b.d.l.	b.d.l.	3.68×10^{-2}	3.76×10^{-2}	5.02×10^{-2}	b.d.l.
1-Pristene	b.d.l.	b.d.l.	b.d.l.	b.d.l.	b.d.l.	b.d.l.	b.d.l.
3,7,11-Trimethyl-1-dococanol	b.d.l.	1.54×10^{-2}	3.23×10^{-4}	3.15×10^{-4}	1.34×10^{-3}	4.20×10^{-3}	4.86×10^{-3}
Durohydroquinone	b.d.l.	b.d.l.	b.d.l.	4.55×10^{-5}	1.50×10^{-5}	2.51×10^{-4}	1.83×10^{-3}
Duroquinone	1.78×10^{-3}	3.38×10^{-2}	5.30×10^{-4}	1.31×10^{-3}	6.62×10^{-4}	b.d.l.	b.d.l.
Total Mass (mg) [b]	0.852	0.143	2.82	11.2	18.8	19.5	0.415

[a] b.d.l.: below detection limit

[b] Total mass of detected compounds on each MOUDI stage